How to cite: *Angew. Chem. Int. Ed.* **2023**, *62*, e202303329
doi.org/10.1002/anie.202303329

Supramolecular Chemistry | Very Important Paper

Dynamic Axial-to-Helical Communication Mechanism in Poly[(allenylethynylenephenylene)acetylene]s under External Stimuli

*María Lago-Silva, María Magdalena Cid, Emilio Quiñoá, and Félix Freire**

Abstract: Helix inversion in chiral dynamic helical polymers is usually achieved by conformational changes at the pendant groups induced through external stimuli. Herein, a different mechanism of helix inversion in poly(phenylacetylene)s (PPAs) is presented, based on the activation/deactivation of supramolecular interactions. We prepared poly[(allenylethynylenephenylene)acetylene]s (PAEPAs) in which the pendant groups are conformationally locked chiral allenes. Therefore, their substituents are placed in specific spatial orientations. As a result, the screw sense of a PAEPA is fixed by the allenyl substituent with the optimal size/distance relationship to the backbone. This helical sense command can be surpassed by supramolecular interactions between another substituent on the allene and appropriate external stimuli, such as amines. So, a helix inversion occurs through a novel axial-to-helical communication mechanism, opening a new scenario for taming the helices of chiral dynamic helical polymers.

Introduction

Dynamic helical polymers have attracted the attention of the scientific community during the last decades due to their stimuli-responsive properties,[1–6] which allow tuning their helical sense[7–9] or elongation,[10–14] once they have been prepared, via external stimuli such as temperature, pH, chiral additives, cations, or anions among others.[15–24] Moreover, helical polymers find applications in other fields such as asymmetric synthesis,[25–27] or chiral stationary phases in High Performance Liquid Chromatography (HPLC),[28,29] due to their structure/function relationship. However, although the secondary structure adopted by a helical polymer is important to establish a correct structure/function relationship, its elucidation is extremely complicated.[30] The main limitation to obtain robust structural data is the presence of monomer repeating units along the polymeric chain, which makes powerful structural techniques such as Nuclear Magnetic Resonance (NMR) practically useless. To obtain an approximate 3D structure of a helical polymer, it is necessary to combine the information obtained from different structural techniques such as Electronic Circular Dichroism (ECD),[31,32] NMR[33,34] and Atomic Force Microscopy (AFM)[35–42] among others.[43] Furthermore, in these systems, chiral information is transmitted from the chiral pendant to the polymeric backbone, such that a handedness preference is induced. In order to rationalize how the stimulus-response is produced, deciphering the operating mechanisms is of utmost importance. In this sense, there are different ways to control the helical sense of a polymer. Thus, if the polymer is chiral, the presence of a preferred conformer at the chiral pendant group results in an induced helical sense that can be either *P* or *M*.[18,44] Variations in the conformational composition of the pendant group result in either helical sense enhancement or helical inversion (Figure 1a).[45,46] On the other hand, if the helical polymer is achiral, amplification of asymmetry phenomena (helical induction) arise from interactions between the polymer and external chiral molecules used as external stimuli.[47] In chiral and achiral polymers, the changes produced in the helical structures are related to the spatial dispositions adopted by the substituents or associated species at the pendant groups. Interestingly, during the last years different mechanisms for the transmission of chiral information have been explored—for example, from the pendant to the polyene backbone in poly(phenylacetylene)s (PPAs)—(Figure 1b).[48–50] In these studies, the chiral pendant group is placed at a remote position, separated from the polyene backbone by achiral spacers. Thus, the helical induction in the polymer can follow two different mechanisms: 1) inducing a conformational change in the achiral spacer[51,7] or 2) inducing a tilting degree in the supramolecular arrangement of the achiral spacers along the helix (Figure 1b).[52] These structural changes produced in the spacer, or in the arrangement of the spacer along the polymer scaffold, are further harvested by the polyene backbone which induces a screw sense excess in the helical material.

Herein, we introduce a novel mechanism of chiral teleinduction by combining two concepts, chirality, and

[*] M. Lago-Silva, Prof. E. Quiñoá, Prof. F. Freire
Centro Singular de Investigación en Química Biolóxica e Materiais Moleculares (CiQUS) and Departamento de Química Orgánica, Universidade de Santiago de Compostela
E-15782 Santiago de Compostela (Spain)
E-mail: felix.freire@usc.es
M. M. Cid
Departamento de Química Orgánica, Universidade de Vigo
36310 Vigo (Spain)

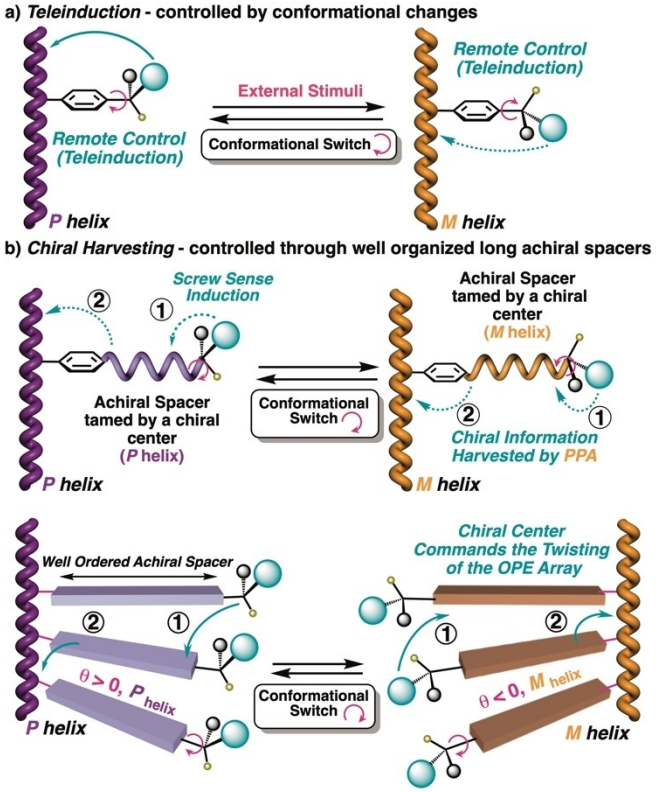

Figure 1. Conceptual representations of the chiral information transmission mechanisms from the pendant to the polyene backbone in PPAs. (a) *Chiral Teleinduction* mechanism. (b) *Chiral Harvesting* mechanism: by inducing a conformational change in the achiral spacer and through a tilting degree in the supramolecular arrangement of the achiral spacers along the helix.

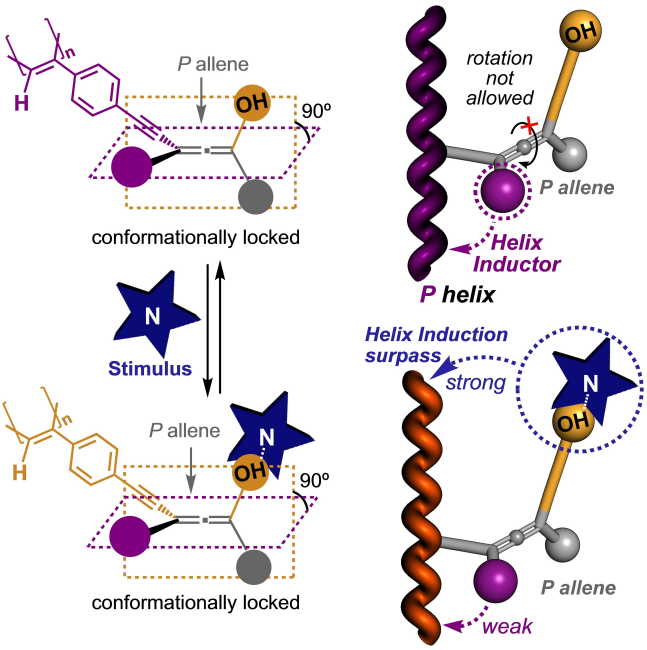

Figure 2. Conceptual view of the chiral information transmission mechanism from the allenic pendants to the polyene backbone via axial-to-helical communication.

supramolecular chemistry to study the direct communication between the polymeric backbone and the chiral pendant. In our design, the idea is to prepare a chiral monomer with a restricted conformational space bearing functional groups that can be involved in supramolecular interactions, such as a properly substituted allenic motif. The restricted rotation in cumulated dienes prevents the relative spatial orientation between the allenic substituents from being altered. So, allenes can possess axial chirality since their four substituents lie in two perpendicular planes (Figure 2). The tunable relative size of the substituents by supramolecular interactions would eventually result in a specific helical handedness in the polymer without altering the conformational composition in the pendant group (Figure 2).

Results and Discussion

To perform these studies, we chose PPAs as helical polymers. The control of the helical sense in PPAs, as already described above, is usually achieved by introducing a chiral center in the monomer repeating unit, where the conformational composition and the distance from the chiral center to the backbone of the polymer plays an important role. In this sense, the polymeric structure (elongation/sense) is related to the different spatial dispositions adopted by the substituents of the chiral pendant. In our design, we envisioned allenes with restricted conformational composition as suitable chiral pendant groups. As a result, the helix adopted by a modified PPA bearing chiral allenes as pendants (i.e., poly[(allenylethynylenephenylene)acetylenes, PAEPAs) should be inert to stimuli that are normally involved in altering the conformational composition of chiral pendants, such as solvent polarity. In this case, a helix inversion can be produced in the PAEPA by taking advantage of the rigidity of the relative spatial orientation between the allenic substituents. We expected that the helical sense of the PPA would be dictated by the relative size of the allenic substituents, with the one closest to the backbone being the key substituent (Figure 2). However, if the allene substituent in a remote position could be involved in supramolecular interactions with other molecules, their joint volume could become large enough to surpass the command of the proximal substituent and cause a helical handedness inversion in the polymer backbone (Figure 2).

For this reason, we focused our attention on 1,3-diethynylallene [(*P*)-**DEA**, (*M*)-**DEA**][53] (Figure 3a). This chiral allene is a highly configurational and stable building block, which displayed outstanding chiroptical properties in the construction of allene-acetylenic oligomers, macrocycles, cages and supramolecular assemblies.[54–60]

Based on this information, we became interested in studying the effect of transferring the molecular properties of allene-acetylenes to the corresponding helical polymers (Figure 2) by exploring a new mechanism of helical induction based on supramolecular interactions between allene and achiral molecules. So, we envisioned phenyl-

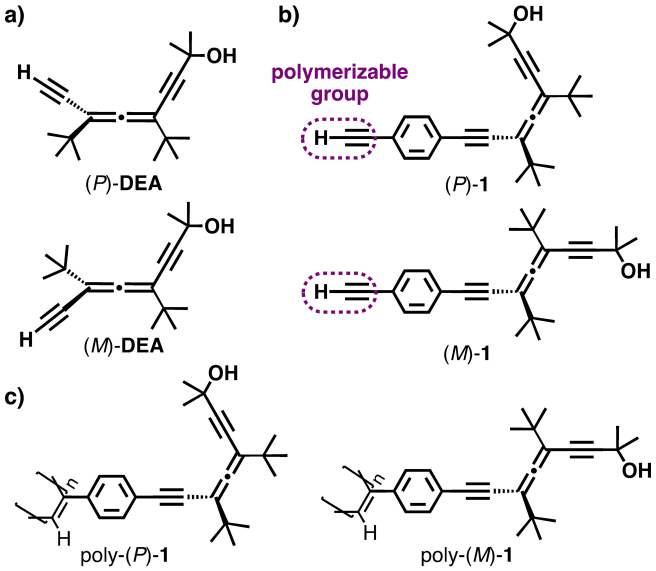

Figure 3. (a) Chemical structure of (*P*)-**DEA** and (*M*)-**DEA**. (b) Chemical structure of monomers (*P*)-**1** and (*M*)-**1**. (c) Chemical structure of polymers poly-(*P*)-**1** and poly-(*M*)-**1**.

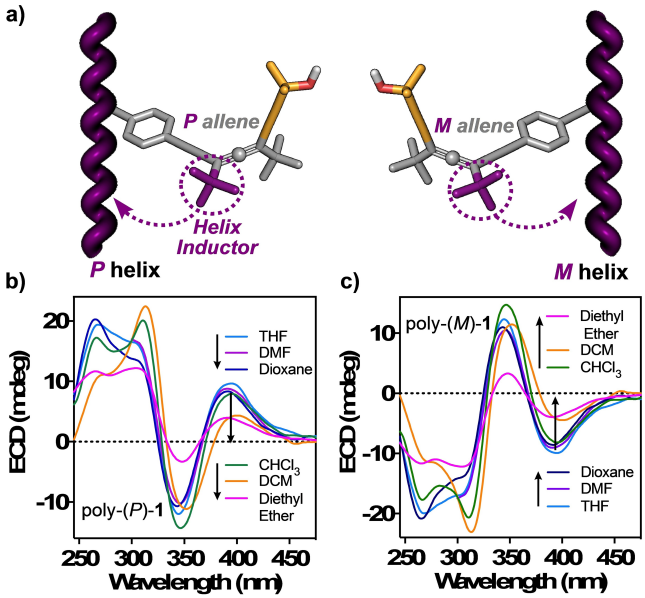

Figure 4. (a) Conceptual view of the chiral information transmission mechanism from the *tert*-butyl group of the allene positioned closest to the polyene backbone via axial-to-helical communication. ECD studies of (b) poly-(*P*)-**1** and (c) poly-(*M*)-**1** in different solvents (0.5 mM).

acetylene monomers bearing (*P*)- and (*M*)-**DEA**—i.e., (*P*)-**1** and (*M*)-**1**—(Figure 3a–b) as suitable building blocks. These allenes have on the carbon located near the polymerizable terminal alkyne, the phenylacetylene group necessary to obtain the polymer and a *tert*-butyl group. These two groups form the first plane while, in the second perpendicular plane, the substituents are *tert*-butyl and 2-methylbut-3-yn-2-ol (Figure 3b). Looking at the structure and considering the rigidity of the chiral allenes used as pendants, one could synthesize a helical polymer (Figure 3c) with a screw sense preference that would be commanded by the *tert*-butyl group placed closest to the backbone (Figure 4a). The other *tert*-butyl and 2-methylbut-3-yn-2-ol substituents would be placed in a more remote position and therefore their helix-inducing effects would be expected to be negligible. However, the hydroxy group in the pendant can establish supramolecular interactions with other molecules via hydrogen bonds, so that the size of the hydroxy-bearing substituent increases without altering its conformational composition. Therefore, this interaction could eventually result in a different helical sense preference with consequent helix inversion (Figure 2).

To test our hypothesis, (*P*)- and (*M*)-**1** monomers were prepared through a Sonogashira cross-coupling between the phenylacetylene derivative and the enantiomerically pure (*P*)- and (*M*)-**DEA** to yield monomers (*P*)-**1** and (*M*)-**1** in ca. 98 % yield (Figure 3b) (**DEA** was prepared according to the literature, see Supporting Information). Next, these monomers were submitted to polymerization using a Rh^{I} catalyst (Figure 3c), which provided poly-(*P*)-**1** and poly-(*M*)-**1** in high yields (98 %) and with high *cis* content of the double bonds[61] as inferred from ^{1}H NMR and Raman spectra (Figures S6 and S8a).

ECD studies of the corresponding polymers in different solvents showed how the helical sense adopted by poly-(*P*)-**1** ($ECD_{390} > 0$, *P* helix) and poly-(*M*)-**1** ($ECD_{390} < 0$, *M* helix) remained unaltered regardless of the donor or polar character of the solvent used to dissolve the polymer (Figures 4b–c). Thus, in these polymers an axial-to-helical induction mechanism arises, where the axial chirality of the allene is transmitted to the polyene backbone through effective teleinduction (Figure 4b–c and S12–14). More precisely, the different spatial orientations of the nearby *tert*-butyl group are those that govern the helical sense of the polymer (Figure 4a). To determine if the DP of the polymer affects its helical properties, a short oligomer of poly-(*P*)-**1** was prepared and stimuli-responsive ECD studies showed that the length of the polymer did not affect its dynamic helical properties (Figures S28–S30).

Next, to demonstrate the axial-to-helical teleinduction surpass mechanism in poly-**1**, we used the hydroxy group of the chiral allene to modify its spatial environment via supramolecular interactions with other molecules, such as amines.

To perform these studies and considering the quasi-static behaviors of poly-(*P*)-**1** and poly-(*M*)-**1** in different solvents, diethyl ether was the solvent of choice to carry them out. In this solvent, poly-(*P*)-**1** and poly-(*M*)-**1** show the least screw sense excess, a fact that indicates a greater dynamic behavior and therefore better stimuli responsive properties (Figure 4b–c). The addition of primary amines such as methylamine, propylamine, isopropylamine, or *tert*-butylamine did not produce helix inversion in poly-(*P*)-**1** (Figure 5a and S16a), even when this PAEPA was dissolved in pure primary amines, where the interaction between poly-(*P*)-**1** and the primary amine was guaranteed (Figure 5b and S15a). The existence of this supramolecular interaction poly-(*P*)-**1**/primary amine was demonstrated by ^{14}N NMR, where

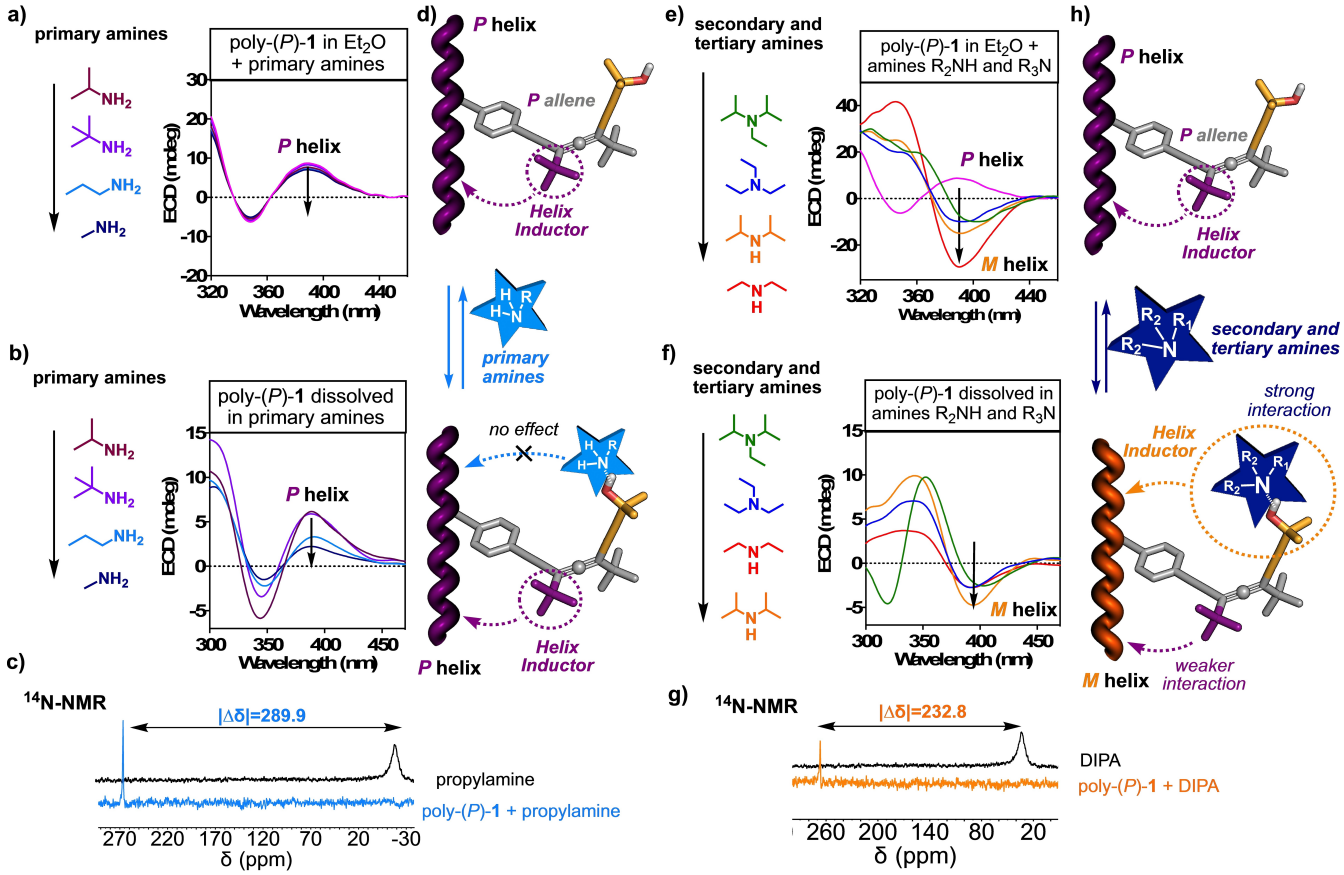

Figure 5. (a) ECD titration experiments of poly-(*P*)-**1** with primary amines in diethyl ether (1.0 mM). (b) ECD studies of poly-(*P*)-**1** dissolved in primary amines (0.3 mM). (c) Comparison of the ^{14}N NMR spectra of methylamine and poly-(*P*)-**1**/methylamine in 1/1 mol/mol ratio (solvent: Et_2O). (d) Conceptual representation of the poly-(*P*)-**1**/primary amine interaction. (e) ECD titration experiments of poly-(*P*)-**1** with secondary and tertiary amines in diethyl ether (1.0 mM). (f) ECD studies of poly-(*P*)-**1** dissolved in secondary or tertiary amines (0.3 mM). (g) Comparison of the ^{14}N NMR spectra of Et_3N and poly-(*P*)-1/Et_3N in a 1/1 mol/mol ratio (solvent: Et_2O). (h) Conceptual representation of the poly-(*P*)-**1**/secondary/tertiary amine interaction.

a shift towards higher frequencies is observed for the N of the amine in a mixture of poly-(*P*)-**1**/primary amine in 1/1 mol/mol ratio (see Figure 5c and S23). Therefore, although the primary amine is attached to PAEPA, the bulkiness around the nitrogen atoms of the primary amines is not sufficient to overcome the effect of the proximal *tert*-butyl group and produce handedness inversion (Figure 5d). Interestingly, when analogous experiments are performed with secondary [e.g., diethylamine, diisopropylamine (DIPA)] and tertiary amines [e.g., triethylamine, diisopropylethylamine (DIPEA)], a helix inversion occurs in poly-(*P*)-**1** (from *P* to *M*, Figure 5e–f, S15b, S16b–d and S17). This helix inversion is not produced by a conformational change in the rigid pendant group, but rather by the supramolecular interaction between the hydroxy group and the amines. This interaction was demonstrated by ^{14}N NMR (Figure 5g and S24–S25). Thus, when the supramolecular interaction poly-(*P*)-**1**/amine (secondary or tertiary) takes place, the volume of the allene substituent that contains the hydroxy group increases and starts to command the helical sense of PAEPA, surpassing the order given by the *tert*-butyl group, which causes a helix inversion (Figure 5h).

As expected, similar results were obtained for poly-(*M*)-**1** due to the enantiomeric relationship, i.e., no response to the presence of primary amines and screw sense inversion from *M* to *P* when secondary or tertiary amines are added to a solution containing poly-(*M*)-**1** (Figures S19 and S20). VT-ECD studies showed the quasi-static behavior of the polymer, where the screw sense excess of the helical polymer could not be altered by temperature changes (Figure S27). However, the helix inversion process is reversible, so that after carrying out a workup with aqueous media to remove the amines, the original helical sense is recovered (Figure S18).

To further demonstrate the role of the hydroxy group in the amine/poly-(*P*)-**1** interaction, its acetylation with acetic anhydride yielded poly-(*P*)-**1-OAc** (Figure 6a). ECD studies in different solvents showed the same *P* helical sense ($ECD_{390} > 0$, *P* helix) as the one adopted by the parent poly-(*P*)-**1** (Figure 6b and S21b). Again, the quasi-static *P* helix adopted by poly-(*P*)-**1-OAc** is attributed to the *P* axial chirality of the allene used as pendant. However, in this case, further addition of amines (primary, secondary, and tertiary) to a diethyl ether solution of poly-(*P*)-**1-OAc** did

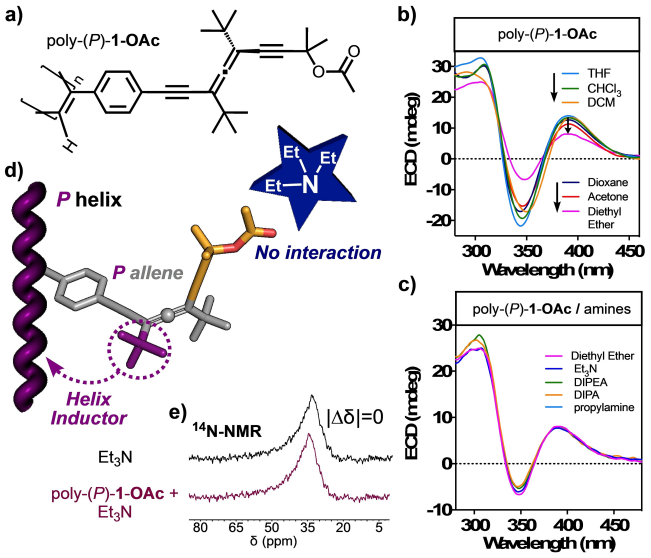

Figure 6. (a) Chemical structure of poly-(*P*)-**1-OAc**. (b) ECD studies of poly-(*P*)-**1-OAc** in different solvents (1.0 mM). (c) ECD studies of different poly-(*P*)-**1-OAc**/amine mixtures in diethyl ether (1.0 mM). (d) Conceptual representation of poly-(*P*)-**1-OAc** screw sense induction. (e) Comparison of the ^{14}N NMR spectra of Et_3N and poly-(*P*)-**1-OAc**/Et_3N in a 1/1 mol/mol ratio (solvent: Et_2O).

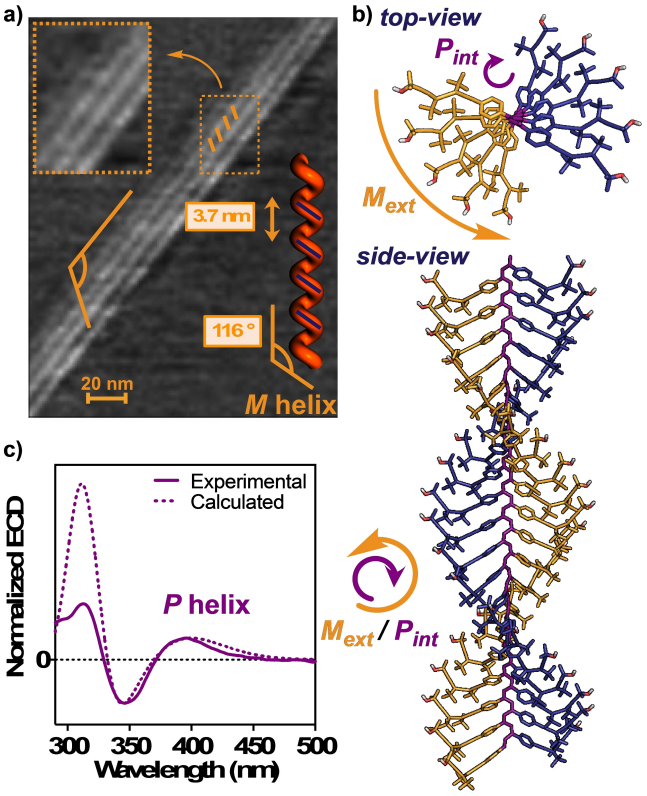

Figure 7. (a) AFM image obtained from a poly-(*P*)-**1** monolayer. (b) 3D model of poly-(*P*)-**1**. (c) ECD spectra of poly-(*P*)-**1** in $CHCl_3$ vs. calculated ECD spectra.

not produce any change in the screw sense preference of the polymer. We attributed this behavior to the lack of interactions between the amines and this PAEPA (Figure 6c and S22). ^{14}N NMR studies corroborate the absence of this supramolecular interaction since the N peak of the amines does not suffer any shift after the addition of poly-(*P*)-**1-OAc** (Figure 6e and S26).

Finally, we aimed to analyze the secondary structure of poly-(*P*)-**1**. Thus, structural studies such as AFM, DSC and computational calculations were carried out. To perform the AFM studies of poly-(*P*)-**1**, it was first necessary to prepare 2D-crystals of these polymers. These crystals were obtained using Yashima's protocol,[36–38] which consist in spin coat a dilute chloroform solution of the polymer onto highly oriented pyrolytic graphite (HOPG) and leaving it under a solvent atmosphere for a few hours. High-resolution AFM images of these crystals were obtained, allowing us to extract several key helical parameters, such as helix width (5 nm), helix pitch (3.7 nm) and the orientation of the external part of the helix (*M* helix) (Figure 7a and S31). Therefore, poly-(*P*)-**1** adopts in chloroform a *cis-transoidal* helix where internal and external helices rotate in opposite directions (Figure 7b). In this case, the polyene backbone rotates clockwise—*P* helix, ($ECD_{390}>0$)—, while the external helix rotates counterclockwise—*M* helix, AFM—. DSC studies corroborated the presence of a *cis-transoidal* polyene skeleton, since a trace with two exothermic peaks was found, typical of this helical scaffold (Figure S9). Combining all the data obtained from the different structural techniques, it was possible to model an approximated 3D structure of poly-(*P*)-**1** ($\omega_1=158°$) (Figure 7b and S32). In addition, TD-DFT (rCAM-B3LYP/3-21G)[62–65] computational studies were carried out for a short oligomer ($n=9$) of poly-(*P*)-**1**, which allowed us to obtain a theoretical ECD spectrum that matches the experimental one (Figure 7c and Supporting Information for more detailed information). This fact indicates that the proposed structure is in good agreement with that adopted by poly-(*P*)-**1** in solution.

Conclusion

We have demonstrated that PAEPAs, which bear chiral and conformationally restricted pendant groups, behave as quasi-static helical polymers, and can be transformed into dynamic helical polymers by on/off (activation/deactivation) supramolecular interactions. Thus, if we can vary the size of the substituents in a conformationally restricted pendant, the order it commands will depend on the activation/deactivation of this supramolecular interaction. This new dynamic mechanism of chiral axial-to-helical communication was demonstrated using poly-(*P*)-**1**, in which a chiral allene with restricted conformational composition plays a key role. In poly-(*P*)-**1**, a *tert*-butyl group commands the helical sense due to its large size and proximity to the backbone. Additional supramolecular interactions between the hydroxy group of a remotely placed allenic substituent with secondary or tertiary amines result in helix inversion in poly-(*P*)-**1** because activation/deactivation of such interactions modifies the relative bulkiness of the dominant

substituents. This dynamic axial-to-helical mechanism was demonstrated by ^{14}N NMR, and by acetylation of the hydroxy group, showing the role of the alcohol/amine interaction on the helix inversion process. These studies open a new window in the design of stimuli-responsive materials, encouraging the scientific community to search for different ways to induce screw sense preferences in helical polymers, as well as to develop new methods of chiral communication in macromolecules.

Acknowledgements

We thank financial support from AEI (PID2019-109733GB-I00, PID2021-128057NB-I00), and Xunta de Galicia (ED431C 2022/21, Centro Singular de Investigación de Galicia acreditación 2019–2022, ED431G 2019/03 and the European Regional Development Fund (ERDF). ML also thanks Xunta de Galicia for a predoctoral contract. We are also thankful for Servicio de Nanotecnología y Análisis de Superficies (CACTI-CINBIO, UVigo) the use of the RIAIDT-USC analytical facilities and CESGA for cpu time.

Conflict of Interest

The authors declare no conflict of interest.

Data Availability Statement

The data that support the findings of this study are available in the supplementary material of this article.

Keywords: Allenes · Axial Chirality · Helix Inversion · Poly(phenylacetylene)s · Stimuli-Responsive

[1] E. Yashima, N. Ousaka, D. Taura, K. Shimomura, T. Ikai, K. Maeda, *Chem. Rev.* **2016**, *116*, 13752–13990.
[2] J. Liu, L. W. Y. Lam, B. Z. Tang, *Chem. Rev.* **2009**, *109*, 5799–5867.
[3] J. Tarrío, R. Rodríguez, B. Fernández, E. Quiñoá, F. Freire, *Angew. Chem. Int. Ed.* **2022**, *61*, e202115070.
[4] E. Yashima, K. Maeda, Y. Furusho, *Acc. Chem. Res.* **2008**, *41*, 1166–1180.
[5] R. Sakai, E. B. Barasa, N. Sakai, S.-I. Sato, T. Satoh, T. Kakuchi, *Macromolecules* **2012**, *45*, 8221–8227.
[6] N. Liu, L. Zhou, Z.-Q. Wu, *Acc. Chem. Res.* **2021**, *54*, 3953–3967.
[7] R. Rodríguez, E. Suárez-Picado, E. Quiñoá, R. Riguera, F. Freire, *Angew. Chem. Int. Ed.* **2020**, *59*, 8616–8622.
[8] R. Rodríguez, E. Rivadulla-Cendal, M. Fernández-Míguez, B. Fernández, K. Maeda, E. Quiñoá, F. Freire, *Angew. Chem. Int. Ed.* **2022**, *61*, e202209953.
[9] L. Xu, Y.-J. Wu, R.-T. Gao, S.-Y. Li, N. Liu, Z.-Q. Wu, *Angew. Chem. Int. Ed.* **2023**, *62*, e202217234.
[10] T. Ikai, R. Ishidate, K. Inoue, K. Kaygisiz, K. Maeda, E. Yashima, *Macromolecules* **2020**, *53*, 973–981.
[11] M. Alzubi, S. Arias, R. Rodríguez, E. Quiñoá, R. Riguera, F. Freire, *Angew. Chem. Int. Ed.* **2019**, *58*, 13365–13369.
[12] R. Rodríguez, E. Quiñoá, R. Riguera, F. Freire, *Chem. Mater.* **2018**, *30*, 2493–2497.
[13] T. Van Leeuwen, G. H. Heideman, D. Zhao, S. J. Wezenberg, B. L. Feringa, *Chem. Commun.* **2017**, *53*, 6393–6396.
[14] M. Alzubi, S. Arias, I. Louzao, E. Quiñoá, R. Riguera, F. Freire, *Chem. Commun.* **2017**, *53*, 8573–8576.
[15] K. Maeda, K. Shimomura, T. Ikai, S. Kanoh, E. Yashima, *Macromolecules* **2017**, *50*, 7801–7806.
[16] S. Arias, F. Freire, M. Calderón, J. Bergueiro, *Angew. Chem. Int. Ed.* **2017**, *56*, 11420–11425.
[17] F. Wang, C. Zhou, K. Liu, J. Yan, W. Li, T. Masuda, A. Zhang, *Macromolecules* **2019**, *52*, 8631–8642.
[18] J. Bergueiro, M. Núñez-Martínez, S. Arias, E. Quiñoá, R. Riguera, F. Freire, *Nanoscale Horiz.* **2020**, *5*, 495–500.
[19] K. Cobos, R. Rodriguez, O. Domarco, B. Fernandez, E. Quiñoá, R. Riguera, F. Freire, *Macromolecules* **2020**, *53*, 3182–3193.
[20] E. Suárez-Picado, E. Quiñoá, R. Riguera, F. Freire, *Angew. Chem. Int. Ed.* **2020**, *59*, 4537–4543.
[21] M. Fukuda, R. Rodríguez, Z. Fernández, T. Nishimura, T. Hirose, G. Watanabe, E. Quiñoá, F. Freire, K. Maeda, *Chem. Commun.* **2019**, *55*, 7906–7909.
[22] Y. Cao, L. Ren, Y. Zhang, X. Lu, X. Zhang, J. Yan, W. Li, T. Masuda, A. Zhang, *Macromolecules* **2021**, *54*, 7621–7631.
[23] S. Leiras, E. Suárez-Picado, E. Quiñoá, R. Riguera, F. Freire, *Giant* **2021**, *7*, 100068.
[24] X.-H. Xu, S.-M. Kang, R.-T. Gao, Z. Chen, N. Liu, Z.-Q. Wu, *Angew. Chem. Int. Ed.* **2023**, *62*, e202300882.
[25] M. Ando, R. Ishidate, T. Ikai, K. Maeda, E. Yashima, *J. Polym. Sci. Part A* **2019**, *57*, 2481–2490.
[26] T. Ikai, M. Ando, M. Ito, R. Ishidate, N. Suzuki, K. Maeda, E. Yashima, *J. Am. Chem. Soc.* **2021**, *143*, 12725–12735.
[27] R. P. Megens, G. Roelfes, *Chem. Eur. J.* **2011**, *17*, 8514–8523.
[28] D. Hirose, A. Isobe, E. Quiñoá, F. Freire, K. Maeda, *J. Am. Chem. Soc.* **2019**, *141*, 8592–8598.
[29] J. Shen, Y. Okamoto, *Chem. Rev.* **2016**, *116*, 1094–1138.
[30] Z. Fernández, B. Fenández, E. Quiñoá, F. Freire, *J. Am. Chem. Soc.* **2021**, *143*, 20962–20969.
[31] J. Tabei, M. Shiotsuki, F. Sanda, T. Masuda, *Macromolecules* **2005**, *38*, 9448–945.
[32] B. Fernández, R. Rodríguez, A. Rizzo, E. Quiñoá, R. Riguera, F. Freire, *Angew. Chem. Int. Ed.* **2018**, *57*, 3666–3670.
[33] C. I. Simionescu, V. Percec, S. Dumitrescu, *J. Polym. Sci. Polym. Chem. Ed.* **1977**, *15*, 2497–2509.
[34] V. Percec, *Polym. Bull.* **1983**, *10*, 1–7.
[35] R. Rodríguez, J. Ignés-Mullol, F. Sagués, E. Quiñoá, R. Riguera, F. Freire, *Nanoscale* **2016**, *8*, 3362–3367.
[36] J. Kumaki, S.-I. Sakurai, E. Yashima, *Chem. Soc. Rev.* **2009**, *38*, 737–746.
[37] S.-I. Sakurai, K. Okoshi, J. Kumaki, E. Yashima, *J. Am. Chem. Soc.* **2006**, *128*, 5650–5651.
[38] S.-I. Sakurai, K. Okoshi, J. Kumaki, E. Yashima, *Angew. Chem. Int. Ed.* **2006**, *45*, 1245–1248.
[39] V. Percec, J. G. Rudick, M. Peterca, S. R. Staley, M. Wagner, M. Obata, C. M. Mitchell, W.-D. Cho, V. S. K. Balagurusamy, J. N. Lowe, M. Glodde, O. Weichold, K. J. Chung, N. Ghionni, S. N. Magonov, P. A. Heiney, *Chem. Eur. J.* **2006**, *12*, 5731–5746.
[40] V. Percec, J. G. Rudick, M. Wagner, M. Obata, C. M. Mitchell, W.-D. Cho, S. N. Magonov, *Macromolecules* **2006**, *39*, 7342–7351.
[41] J. G. Rudick, V. Percec, *Macromol. Chem. Phys.* **2008**, *209*, 1759–1768.
[42] V. Percec, M. Obata, J. G. Rudick, B. B. De, M. Glodde, T. K. Bera, S. N. Magonov, V. S. K. Balagurusamy, P. A. Heiney, *J. Polym. Sci. Part A* **2002**, *40*, 3509–3533.

[43] B. Nieto-Ortega, R. Rodríguez, S. Medina, E. Quiñoá, R. Riguera, J. Casado, F. Freire, F. J. Ramírez, *J. Phys. Chem. Lett.* **2018**, *9*, 2266–2270.
[44] S. Arias, M. Núñez-Martínez, E. Quiñoá, R. Riguera, F. Freire, *Small* **2017**, *13*, 1602398.
[45] J. J. L. M. Cornelissen, A. E. Rowan, R. J. M. Nolte, N. A. J. M. Sommerdijk, *Chem. Rev.* **2001**, *101*, 4039–4070.
[46] R. Rodríguez, E. Quiñoá, R. Riguera, F. Freire, *J. Am. Chem. Soc.* **2016**, *138*, 9620–9628.
[47] E. Yashima, K. Maeda, Y. Okamoto, *Nature* **1999**, *399*, 449–451.
[48] K. Cobos, E. Quiñoá, R. Riguera, F. Freire, *J. Am. Chem. Soc.* **2018**, *140*, 12239–12246.
[49] S. Arias, R. Rodríguez, E. Quiñoá, R. Riguera, F. Freire, *J. Am. Chem. Soc.* **2018**, *140*, 667–674.
[50] Y. Nagata, T. Nishikawa, M. Suginome, *ACS Macro Lett.* **2016**, *5*, 519–522.
[51] Y.-Z. Ke, Y. Nagata, T. Yamada, M. Suginome, *Angew. Chem. Int. Ed.* **2015**, *54*, 9333–9337.
[52] Z. Fernández, B. Fernández, E. Quiñoá, R. Riguera, F. Freire, *Chem. Sci.* **2020**, *11*, 7182–7187.
[53] S. Odermatt, J.-L. Alonso-Gómez, P. Seiler, M. M. Cid, F. Diederich, *Angew. Chem. Int. Ed.* **2005**, *44*, 5074–5078.
[54] P. Rivera-Fuentes, J.-L. Alonso-Gómez, A. G. Petrovic, F. Santoro, N. Harada, N. Berova, F. Diederich, *Angew. Chem. Int. Ed.* **2010**, *49*, 2247–2250.
[55] J.-L. Alonso-Gómez, P. Rivera-Fuentes, N. Harada, N. Berova, F. Diederich, *Angew. Chem. Int. Ed.* **2009**, *48*, 5545–5548.
[56] S. Castro-Fernandez, I. R. Lahoz, A. Llamas-Saiz, J.-L. Alonso-Gómez, M. M. Cid, A. Navarro-Vázquez, *Org. Lett.* **2014**, *16*, 1136–1139.
[57] C. Gropp, N. Trapp, F. Diederich, *Angew. Chem. Int. Ed.* **2016**, *55*, 14444–14449.
[58] F. W. Goetzke, C. Gropp, A. Schwab, J. E. Donckèle, C. Thilgen, F. Diederich, *Helv. Chim. Acta* **2022**, *105*, e202200130.
[59] P. Rivera-Fuentes, F. Diederich, *Angew. Chem. Int. Ed.* **2012**, *51*, 2818–2828.
[60] S. Míguez-Lago, B. D. Gliemann, M. Kivala, M. M. Cid, *Chem. Eur. J.* **2021**, *27*, 13352–13357.
[61] C. I. Simionescu, V. Percec, *Prog. Polym. Sci.* **1982**, *8*, 133–214.
[62] B. Fernández, R. Rodríguez, E. Quiñoá, R. Riguera, F. Freire, *ACS Omega* **2019**, *4*, 5233–5240.
[63] E. Runge, E. K. U. Gross, *Phys. Rev. Lett.* **1984**, *52*, 997–1000.
[64] Y. Yanai, D. P. Tew, N. C. Handy, *Chem. Phys. Lett.* **2004**, *393*, 51–57.
[65] J. S. Binkley, J. A. Pople, W. J. Hehre, *J. Am. Chem. Soc.* **1980**, *102*, 939–947.

Manuscript received: March 6, 2023
Accepted manuscript online: May 22, 2023
Version of record online: June 12, 2023